# Focusing and Mobilization of Bacteria in Capillary Electrophoresis

**ARTICLE** *in* ANALYTICAL CHEMISTRY · MARCH 2011

Impact Factor: 5.64 · DOI: 10.1021/ac1023815 · Source: PubMed

analytical chemistry

ARTICLE

pubs.acs.org/ac

# Focusing and Mobilization of Bacteria in Capillary Electrophoresis

Farid Oukacine,[†,‡] Laurent Garrelly,[‡] Bernard Romestand,[§] David M. Goodall,[∥] Tao Zou,[†] and Hervé Cottet*[,†]

[†]Institut des Biomolécules Max Mousseron (IBMM, UMR 5247 CNRS-Université de Montpellier 1—Laboratoire Ecosystèmes Lagunaires), Place Eugène Bataillon, CC 1706, 34095 Montpellier Cedex 5, France

[‡]COLCOM, Cap Alpha Avenue de l'Europe, Clapiers 34940 Montpellier, France

[§]Laboratoire Ecosystèmes Lagunaires, UMR 5119, Université de Montpellier 2, 34095 Montpellier, France

[∥]Paraytec Ltd., 1a St Georges Place, York YO24 1GN, United Kingdom

**ABSTRACT:** An isotachophoretic method has been developed for mobilizing and focusing bacteria. This allows quantification and detection of bacteria in a narrow zone. Very good linearity was obtained for *Micrococcus lysodeikticus* (also called *Micrococcus luteus*, studied as a model of Gram+ bacteria) in the range of $0.4 \times 10^8$ cells/mL to $2.9 \times 10^8$ cells/mL, with correlation coefficients for peak height and peak area as a function of cell concentration of 0.999 and 0.998, respectively. This method is usable on both bare and hydroxypropyl cellulose-coated fused silica capillaries. The best results were obtained using 13.6 mM Tris, 150 mM boric acid as terminating electrolyte, and 4.5 mM Tris, 50 mM boric acid, and 3.31 mM HCl as leading electrolyte. With a 33.5 cm ×100 $\mu$m i.d. capillary, short migration times were obtained while maintaining very low electrical current in order to minimize any Joule heating and lysis of the bacteria. A UV area imaging detector (ActiPix D100, Paraytec) was used with a 109 cm × 100 $\mu$m i.d. capillary having three loops and four detection windows to monitor the migration behavior of *M. luteus* and to show the stability of the zone of the focused bacteria along the capillary. Similar results were obtained for *Erwinia carotovora* (a model of Gram− bacteria), and for *Enterobacter cloacae* and *Vibrio splendidus*.

Infectious diseases are caused by pathogenic microorganisms such as bacteria, viruses, and fungi. Some bacteria can cause severe diseases, for example tuberculosis, cholera, and leprosy. According to a report by the World Health Organization (WHO), infectious diseases are now the leading cause of mortality among children and young adults. They are responsible for more than 13 million deaths each year and for one in two deaths in developing countries.[1] Transmission is usually via the fecal/oral route with ingestion of the pathogen in contaminated food or water. For example, cholera is an acute diarrheal infection caused by ingestion of the bacterium *Vibrio cholerae*. The extremely short incubation period, two hours to five days, enhances the potentially explosive pattern of outbreaks, as the number of cases can rise very quickly.[2] In some cases contamination by inhalation is also observed. Thus, Legionellosis is a generic term describing the pneumonic and nonpneumonic forms of infection with *Legionella*. *Legionella* organisms can be spread by aerosols transported by the wind. Infection results from inhalation of contaminated water sprays or mists.[3]

A variety of techniques exist for the analysis of microorganisms. These techniques include differential staining, serological methods, flow cytometry, phage typing, protein analysis, comparison of DNA nucleotide sequences, and surface plasmon resonance.[4] Unfortunately, many of these procedures require the preparation of bacterial cultures, which dramatically lengthens the analysis time,[5] and there is still no way to provide definitive identification of unknown bacteria within a single test. A typical assay may last more than 70 h, including a series of steps such as selective enrichment, biochemical screening, and serological confirmation.[6] Thus, rapid identification, quantification, and characterization of bacterial contamination in water, food, and biological samples without isolation of pure cultures plays a very important role in the field of public health.

Hjertén et al.[7] were the first to introduce the idea of microbial analysis by capillary electrophoresis (CE). They showed that tobacco mosaic virus and *Lactobacillus casei* migrated through a capillary and proved that the orientation of tobacco mosaic virus affected its electrophoretic mobility. However, there was no separation of the different species of microorganisms because all of the bacteria moved together with the electroosmotic flow. Subsequently, research efforts have been carried out to develop rapid methods for identification and quantification of microorganisms by CE.[8−11] In 1999, Armstrong reported a novel CE method for highly efficient separation of mixtures of several species of bacteria.[12] This technique involves the capillary zone electrophoresis of the bacteria using a TBE (Tris/boric acid/ethylenediaminetetraacetic acid (EDTA)) pH 8.4 buffer solution containing 0.0125% poly(ethylene oxide) (PEO) in a bare, fused silica capillary with UV absorbance detection. This method based on TBE buffer including PEO has been widely used in the past decade for the separation of different bacteria[9,12−14] or for the detection of microbial food contaminants (see review[14]). High efficiencies were achieved under optimized conditions.[15] Shintani et al. demonstrated a similar technique when using a carbohydrate polymer additive instead of PEO.[16] However, because of the instability of microbial aggregates, this method

**Received:** September 7, 2010
**Accepted:** November 22, 2010
**Published:** January 04, 2011

leads in some case to multiple small peaks.[17−19] Yu et al. used large volume sample stacking (LVSS) with polarity switching for the analysis of bacteria by CE.[17] With the focusing effect, bacterial cells including single cells, clusters, and aggregates underwent complete focusing and formed a large combined sample zone during migration. Because electroosmotic flow (EOF) is necessary to provide focusing of bacteria, LVSS is not possible using coated capillaries where EOF is suppressed. Rodriguez et al. used CE in conjunction with surfactant (CTAB), which serves to temporally reverse the migration direction of the cells. Another segment with a blocking agent serves to stop the cell migration and to focus them into a narrow zone.[20] Since a high concentration of CTAB may lyse the cells, dicationic ionic liquids were used as auxiliary buffer additives for lowering the required CTAB concentration.[21] Petr et al. have explored several other preconcentration techniques such as pH-induced stacking and normal stacking mode for the analysis of *S. subterranea*.[22] Another approach uses capillary isoelectric focusing (cIEF) to separate bacteria by their surface charge or isoelectric point.[12,23] Generally, in cIEF, sodium hydroxide and phosphoric acid are used as the catholyte and anolyte, respectively, in a coated capillary.

The aim of this work is to develop a new CE method that allows detection and quantification of bacteria in a single peak of high efficiency without multiple peaks attributable to irregular clusters and aggregates of bacterial cells. This method is designed to be usable on both bare and coated (hydroxypropyl cellulose) fused silica capillaries at close to physiological pH, and does not require addition of any polymer additive, surfactant, or strong complexing reagent such as EDTA. Four genera of bacteria have been studied (*Micrococcus luteus*, *Enterobacter cloacae*, *Erwinia carotovora*, and *Vibrio splendidus*).

## EXPERIMENTAL SECTION

**Chemicals.** Boric acid 99.999% ($H_3BO_3$), Tris 99.9% $(HOCH_2)_3CNH_2$, hydrochloric acid 99.999%, benzoic acid ($C_7H_6O_2$), anthraquinone-1,5-disulfonic acid disodium salt ($C_{14}H_6O_8S_2Na_2$), anthraquinone-2-sulfonic acid sodium salt ($C_{14}H_9O_6SNa$), sodium phosphate dibasic ($Na_2HPO_4$), and hydroxypropyl cellulose ($M_w$ 100 000 g/mol) were purchased from Aldrich (Steinheim, Germany). Sodium hydroxide (NaOH) was from VWR (Leuven, Belgium). Deionized water was further purified with a Milli-Q system from Millipore (Molsheim, France). ATP biomass Kit HS was purchased from BioThema (Henden, Sweden) and BacTiter-Glo from Promega (Charbonnières, France). The nutrient broth medium was purchased from Difco Laboratories (Franklin Lakes, NJ). The Luria−Bertani (LB) agar plates, the Zobell's agar plates, and the bacteria *Micrococcus luteus* ATCC 4698, *Vibrio splendidus* LGP32, *Enterobacter cloacae*, and *Erwinia carotovora* (from IBMC Strasbourg collection) were kindly donated by the Lagoon Ecosystems laboratory, Université Montpellier 2 (Montpellier, France).

**Bacterial Growth Conditions and Sample Preparation.** The different bacterial species were maintained under strictly controlled growth conditions: the starting culture colonies of the bacteria (*M. luteus*, *E. cloacae*, and *E. cartotovora*) were transferred from LB agar plates into Erlenmeyer flasks containing 8 mL of LB liquid medium. *V. splendidus* was transferred from Zobell's agar plates into Erlenmeyer flasks containing the same volume of Zobell's liquid medium. The flasks were incubated for 13 h at 30 °C with constant agitation (120 rpm) on a rotary platform shaker for good aeration. The fresh liquid cultures were prepared daily. To separate the bacteria from the medium, the suspension in the flasks was centrifuged (model: Sigma3K12, Sigma Laborzentrifugen, Osterode, Germany) at 6000 rpm for 5 min to get the bacteria in pellet form. The supernatant was removed carefully, and the pellet was resuspended in 8 mL of CE buffer by vortexing for 1 min. Then the bacterial suspension was centrifuged again for 5 min. This washing process was repeated twice. Eight milliliters of CE buffer was added to the washed bacterial cells, and the solution was vortexed until the pellets were resuspended completely. Next, the bacterial suspensions were stored at 4 °C. Before use, filtration of the buffer is required to remove any possible bacterial contamination from the buffer. The filtration was performed using MF-Millipore Filters with 0.45 $\mu$m pore size (Millipore SAS, Molsheim, France). Cell concentrations of bacteria were determined by cellular ATP measurement. The principle of the measurement relies on the count of photons produced by the action of an enzyme (luciferase)-emitting photons in the process of hydrolysis of an ATP molecule:

$$\mathrm{ATP} + \mathrm{luciferin} + \mathrm{O_2} \xrightarrow[\text{luciferase}]{\mathrm{Mg^{++}}} \mathrm{AMP} + \mathrm{PP_i} + \text{oxyluciferin} + \text{light}$$

where ATP is adenosine triphosphate, AMP is adenosine monophosphate, and $PP_i$ is pyrophosphate ($P_2O_7^{4-}$). This phenomenon is called bioluminescence. The intensity of emitted light was measured with a luminometer (Kikkoman Lumitester C-110, Isogen Life Science, De Meern, The Netherlands). For the quantification of bacteria, two types of ATP can be differentiated: the intracellular ATP (iATP) corresponding to living organisms and the extracellular ATP (eATP) corresponding to dead organisms or bacteria. Total ATP (tATP) is the sum of iATP and eATP. The extracellular ATP in the bacterial sample was quantified using a reagent (ATP biomass Kit HS) containing luciferin, $Mg^{2+}$, and luciferase. Total ATP was quantified using a second reagent (BacTiter-Glo), which contains the same compounds as those previously mentioned and a lysis solution containing DDAB (didecyldimethylammonium bromide), Triton X-100, chlorhexidine, and EDTA. Subtraction of the amount of eATP from the amount of total ATP allows the determination of the amount of intracellular ATP. This measure is directly proportional to the active biomass: there is a consensus that 1 pg of ATP corresponds to 1000 microorganisms.[24]

**Capillary Coating.** The hydroxypropyl cellulose (HPC)-coated capillaries have been prepared according to a literature protocol.[25,26] The HPC powder was dissolved at room temperature in water to a final concentration of 5% (w/w). The polymer solutions were left overnight to eliminate bubbles. The capillary columns were filled with the polymer solution using a syringe pump (KDS100, Holliston, USA) for 30 min, and the excess of polymer solution was removed using $N_2$ gas at 3 bar for a 50 $\mu$m i.d. capillary, and 0.25 bar for a 100 $\mu$m i.d. capillary. The HPC polymer layer was immobilized by heating the capillary in a GC oven (GC-14A, Shimadzu, France) at 60 °C for 10 min and using a linear ramp from 60 to 140 °C at 5 °C/min, and finally 140 °C for 20 min, keeping $N_2$ pressure at 3 bar or at 0.25 bar depending on the i.d. of the capillary. Before use, the coated capillaries were rinsed with water for 10 min. At the end of each day, the HPC-coated capillary was flushed with water for 10 min and with air for 5 min. The coated capillary was found to be stable during more

than 150 injections of bacteria (i.e., 15 injections per day for 2 weeks).

**Capillary Electrophoresis.** CE experiments were carried out with a 3D-CE instrument (Agilent Technologies, Waldbronn, Germany) equipped with a diode array detector. Separation capillaries prepared from bare, fused silica tubing were purchased from Composite Metal Services (Shipley, UK). New fused silica capillaries were conditioned by performing the following washes: 1 M NaOH for 20 min, 0.1 M NaOH for 15 min, and water for 10 min. The temperature of the capillary cassette was maintained constant at 25 °C. Samples were injected hydrodynamically.

**UV Area Imaging Detection.** Imaging experiments and detection at multiple windows in a looped capillary were carried out with an ActiPix D100 UV area imaging detector (Paraytec, York, UK). The detector uses a 9 mm × 7 mm active pixel sensor array made up of 1280 × 1024 individual 7 $\mu$m pixels. Pixel binning by a factor 10 in the row dimension parallel to the axis of the capillary gives 128 × 1024 effective pixels. Each column of effective pixels provides zones for both sample and reference, and this self-referencing process ensures good signal-to-noise ratios independent of any fluctuations in light source intensity.[27] The light source was a pulsed xenon light source, and wavelength selection was via a 280 nm interference filter with 10 nm bandpass (full width at half-maximum). In the image mode, intensity counts at all effective pixels are stored for all frames. This mode was used for imaging a zone of bacteria traversing a capillary window. The frame rate used was 2.815 Hz. Image data were postprocessed in frame mode using a cartridge map with a sample zone width of 100 $\mu$m in the direction transverse to the capillary axis; alteration of the cartridge map to vary the width of the sample zone, in the range 7−120 $\mu$m, was found to have no effect on the results for peak width and velocity. A constant velocity is initially estimated and optimized during postprocessing of frame data by a peak height maximization routine. When all frames are superposed and averaged with time displacements corresponding to the optimum velocity, the peak width is minimized and the height maximized. A further benefit of frame averaging in this way is that analyte signals are correlated, whereas the noise is uncorrelated; the net result is a gain in signal-to-noise ratio proportional to the square root of the number of frames averaged during traversal of the array. For other experiments, data were typically collected in frame or trace mode in order to reduce data file size. The frame rate used was 10 Hz. Here the signals are preprocessed with an algorithm which computes appropriate time displacements to add together and average the snapshots. For CZE, the velocity is calculated in the software from the length and time to the detector window. Imaging at four detection windows was carried out as described elsewhere.[28]

**ITP Computer Simulation.** For simulations of the isotachophoretic process, the freeware program Simul 5.0 by Gaš et al.[29] was used. The Simul 5.0 software is available as freeware at http://natur.cuni.cz/gas. The simulation was performed with 1000 grid points along a 25 mm long separation space for a 1 mm long sample zone, 2 mm long inlet zone, and 23 mm long outlet zone. Simulation was performed at a constant voltage of −250 V and without electroosmotic flow. The inner diameter of the capillary is 50 $\mu$m, and the optimization interval was 100 steps.

## RESULTS AND DISCUSSION

**Separation of Bacteria Using CZE.** Figure 1 displays the results of three successive injections of *M. luteus* (Gram+)

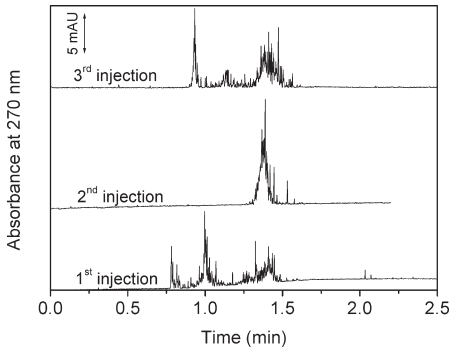


**Figure 1.** Electropherograms of three successive injections of *M. luteus* by CZE in system A (see Table 1). Experimental conditions: Fused silica capillary 33.5 cm (25 cm to the detector) × 100 $\mu$m i.d. Electrolyte: Tris 4.5 mM, boric acid 50 mM. Applied voltage: +20 kV. Hydrodynamic injection: 17 mbar, 6 s. Sample: *M. luteus* at 2.5 × $10^8$ cells/mL diluted in the separation buffer. Other conditions as described in Capillary Electrophoresis.

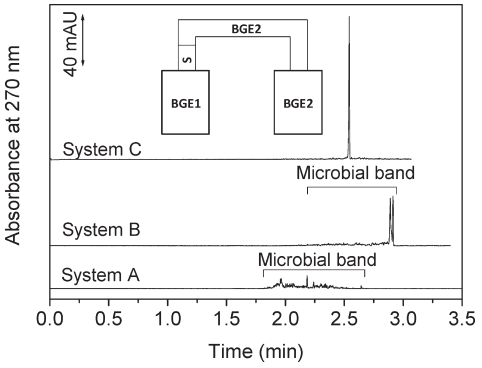


**Figure 2.** Electrophoregrams of *M. luteus* for different BGE systems. Experimental conditions: Fused silica capillary, 33.5 cm (25 cm to the detector) × 100 $\mu$m i.d. Electrolytes: as indicated on the figure (see Table 1 for BGE compositions). Applied voltage: +15 kV. Hydrodynamic injection: 17 mbar, 6 s. Sample: *M. luteus* at 2.5 × $10^8$ cells/mL diluted in Tris (4.5 mM) boric acid (50 mM) buffer. Insert: schematic showing compositions of inlet and outlet vials and capillary at the beginning of the experiment.

obtained in CZE in a Tris-borate buffer. Multiple small peaks having different electrophoretic mobilities were observed. These small peaks correspond to clusters and/or aggregates of different sizes. Similar results were obtained for bacillus species such as *E. cloacae* (Gram−), *E. carotovora* (Gram−), and for *V. splendidus* (data not shown). In this mode, the formation of microbial aggregates during the electrophoretic process renders it impossible to use CZE for reproducible and quantitative analysis of bacteria. In a previous CZE study, using the rod-shaped *Bifidobacterium infantis* (bacillus species), Zheng et al. proposed a collision-based aggregation mechanism in which collisions between microbes result from different mobilities and migration directions in the electric field.[30] A similar explanation could hold for observations in the current study. *M. luteus* is a Gram positive, spherical bacterium, that belongs to the family *Micrococcaceae*.[31] Despite the spherical form of *M. luteus*, binary fission used by prokaryotic organisms for their reproduction leads to nonuniform shapes of bacteria in the solution. So, when an electric field is applied, bacteria migrate with different velocities according to

**Table 1. BGE Compositions Used in This Work, Calculated pH and Ionic Concentrations (values in parentheses) of $TrisH^+$, $B(OH)_4^-$, $Cl^-$. BGE1 and BGE2 Correspond Respectively to the Electrolyte Present in the Inlet and Outlet Vials (see insert in Figure 2)**

| | BGE1 (concentrations in mM) | | | | BGE2 (concentrations in mM) | | | |
|---|---|---|---|---|---|---|---|---|
| | Tris | boric acid | HCl | pH | Tris | boric acid | HCl | pH |
| system A | 4.5 (2.61) | 50 (2.61) | 0 | 7.95 | 4.5 (2.61) | 50 (2.61) | 0 | 7.95 |
| system B | 4.5 (3.20) | 50 (1.53) | 1.67 (1.67) | 7.70 | 4.5 (2.61) | 50 (2.61) | 0 | 7.95 |
| system C | 4.5 (3.90) | 50 (0.60) | 3.31 (3.31) | 7.28 | 4.5 (2.61) | 50 (2.61) | 0 | 7.95 |
| system D | 13.6 (8.08) | 150 (8.08) | 0 | 7.94 | 4.5 (3.90) | 50 (0.60) | 3.31 (3.31) | 7.28 |
| system E (inverted system C) | 4.5 (2.61) | 50 (2.61) | 0 | 7.95 | 4.5 (3.90) | 50 (0.60) | 3.31 (3.31) | 7.28 |

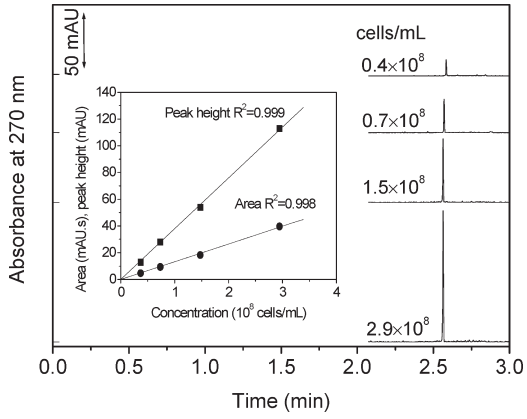


**Figure 3.** Quantification of *M. luteus* suspension in system C on a fused silica capillary. Experimental conditions: Fused silica capillary 33.5 cm (25 cm to the detector) × 100 μm i.d. Electrolyte: system C (see table 1 for BGE composition). Hydrodynamic injection: 17 mbar, 6 s. Applied voltage: +15 kV. Sample: *M. luteus* diluted in Tris (4.5 mM) boric acid (50 mM) buffer. Cell concentrations are shown on the figure.

their different sizes and to their different drag coefficients. Collisions between bacteria lead to larger clusters/aggregates. Because of their increased cross-sectional area, the aggregates have a higher chance of colliding with other isolated microbes or with other aggregates.[32]

**From CZE to the Focusing of Bacteria in Fused Silica Capillaries.** A number of different CE approaches have been reported in a effort to control the process of aggregation of bacteria in the capillary in order to improve the reproducibility, selectivity, and sensitivity of microbial analysis.[12,16,17,20,22,23] We observed that when a small amount of HCl was added to the inlet vial buffer, the electrophoretic profile was greatly improved. Figure 2 shows the effects on the electropherograms of *M. luteus* when HCl was added to the inlet vial (A, no HCl; B, 1.67 mM; C, 3.31 mM). The exact BGE compositions of the different systems are described in Table 1, and the position of the electrolytes in the vials and in the capillary are depicted in the insert of Figure 2. Figure 2 (system A) shows that in the absence of HCl in the inlet vial, multiple peaks were detected as previously described. When the HCl concentration in the vial was increased (systems B and C), the band of bacteria was focused, leading to a dominant sharp peak at 3.31 mM HCl with an efficiency approaching 600 000 plates $m^{-1}$. Under these conditions, a focusing effect allows the bacterial cells to migrate in a single zone. Figure 3 shows the calibration curve for the quantification of *M. luteus* in system C. It can be seen that very good linearity was obtained under these electrophoretic conditions in the range of $0.4 \times 10^8$ cells/mL to $2.9 \times 10^8$ cells/mL. For peak height and for peak area, the correlation coefficients obtained are 0.999 and 0.998, respectively. Note that cell concentrations were determined via the quantification of ATP in the samples (see Bacterial Growth Conditions and Sample Preparation).

**Determination of the Mechanism of Focusing of Bacteria.** To elucidate the focusing mechanism that allowed good linearity to be obtained in the quantification of bacteria using system C, the main differences between the two compartments (at the inlet and at the outlet of the capillary) were considered. There are differences in the pH between the two compartments (7.28 and 7.95 at the inlet and at the outlet of the capillary, respectively), presence of chloride ions in the inlet of the capillary, and slightly higher concentration of borate anions ($B(OH)_4^-$) in the outlet of the capillary. pH values and concentrations of $B(OH)_4^-$ and $TrisH^+$ were calculated using the constraint of electroneutrality, and as in ref 33 from the boric acid, Tris, and HCl concentrations (see Table 1), the $pK_a$ values[34] at 25 °C (boric acid 9.23, Tris 8.06), with activity coefficients of borate and $TrisH^+$, were evaluated using the Debye−Hückel limiting law, applicable at the low ionic strengths of the solutions. The first possible explanation considered is the mechanism of pH junction (see ref 35 for more details) related to the difference in pH between the two compartments. It is well-known that bacteria are amphoteric species. However, the isoelectric point, p*I*, of most bacterial cells lies within the pH range of 1.5−4.5.[36,37] At the pH values of 7.28 and 7.95 calculated for system C, the bacterial cells are negatively charged and the difference in pH would be expected to contribute only to a small change in mobility at the boundary between BGE1 and BGE2 and cannot alone explain the focusing mechanism. The second possibility considered is the mechanism of ITP, where chloride ions act as leading ions and borate ions act as terminating ions. Though the concentration in borate under all forms is the same in both compartments (50 mM), the concentration of borate ion is higher in the outlet than in the inlet capillary because of the HCl present in BGE1 but not BGE2; borate ion concentrations were calculated to be 2.61 mM in the outlet (terminating) vial and 0.60 mM in the inlet (leading) vial (Table 1).

Since ITP is generally performed under suppressed EOF conditions[38] and with constant current[39] to minimize zone-broadening due to any EOF mismatch arising from variations in the composition of samples zones, *M. luteus* was analyzed in a hydroxypropyl cellulose (HPC)-coated capillary with reversed polarity and at constant current (typically 3 μA). The EOF mobility was determined using the Vigh method[40] as $0.10 \times 10^{-9}$ $m^2$ $V^{-1}$ $s^{-1}$. For this study, a UV area imaging detector


dx.doi.org/10.1021/ac1023815 |*Anal. Chem.* 2011, 83, 1571–1578

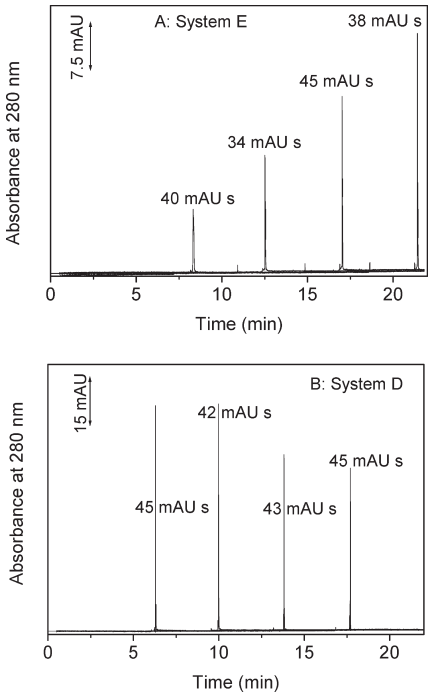


**Figure 4.** Electropherograms of *M. luteus* with four detection points in BGE system E (A) and BGE system D (B). Experimental conditions: Hydroxypropyl cellulose (HPC)-coated capillary 109 cm with three loops and four detection windows (27.5 cm to the 1st, 42.5 cm to the 2nd, 57.5 cm to the 3rd, and 72.5 cm to the 4th detection window) × 100 $\mu$m i.d. BGEs: system E (A), system D (B); see Table 1 for BGE compositions. Applied current: 3 $\mu$A. Hydrodynamic injection: 50 mbar, 7 s. Sample: *M. luteus* at 2.5 × $10^8$ cells/mL diluted in 4.5 mM Tris, 50 mM boric acid (A); 13.6 mM Tris, 150 mM boric acid (B). Multiplexed detection using ActiPix D100 UV area imaging detector at 280 nm.

(ActiPix D100) was used with a capillary having three loops and four detection windows placed at 27.5, 42.5, 57.5, and 72.5 cm from the inlet capillary end. This allowed the migration behavior of *M. luteus* to be monitored at multiple time points in a single run. Figure 4A shows the electrophoretic profiles of *M. luteus* obtained in system E (see table 1). Here the inlet electrolyte (terminating) is constituted by 4.5 mM Tris and 50 mM boric acid, and the outlet electrolyte (leading) is constituted by 4.5 mM Tris, 50 mM boric acid, and 3.31 mM HCl. Compositions of the electrolytes are similar to system C, but BGE1 and BGE2 are reversed, corresponding to the reversal of polarity required to drive the anions toward the detection zone in a coated capillary with zero EOF. In Figure 4A, although the peak area remains effectively constant (~40 mAU s) at all four windows, the peak height increases. This indicates that the peaks are narrowing with increasing time, and that an ITP equilibrium has not been reached. In order to test whether isotachophoresis was indeed the mechanism leading to the focusing effect, with chloride ions acting as leading electrolyte and borate ions as terminating electrolyte, the concentrations of buffer components in the inlet vial were increased by a factor of 3. Figure 4B shows the electrophoretic profiles of *M. luteus* viewed at the four detection windows using system D, with the inlet (terminating) electrolyte constituted by 13.6 mM Tris and 150 mM boric acid and keeping constant the composition of the outlet (leading) electrolyte as in system E (4.5 mM Tris, 50 mM boric acid, and 3.31 mM HCl). Under these conditions, both the peak areas and peak heights remain constant within the uncertainty of the measurements at all four detection windows, i.e., during all the electrophoretic process, showing that the steady state was reached before the first detection window. In a series of experiments (data not shown) designed to investigate the repeatability for *M. luteus* with electrolyte system D, the HP-3D CE was used with a 100 $\mu$m i.d. HPC coated capillary (65 cm length, 56.5 cm to the detector). Good repeatability was obtained, with $RSD_{(n=7)}$ values on peak area and migration time 4.8% and 1.1%, respectively.

In experiments described thus far with the UV area imaging detector, data were obtained in trace mode. In this mode, individual snapshots taken while the zones traverse the length of an imaging window are preprocessed as described in UV Area Imaging Detection, and results are reported as traces of absorbance versus time. In order to provide increased detail of the migrating bacterial zone, an experiment was carried out with the ActiPix D100 in imaging mode. Here all individual snapshots are recorded and give details of absorbance in the capillary at each effective pixel. Figure 5 shows a sequence of images and results of processing frames of the bacterial zone traversing the 9 mm length of the first imaging window. The frame rate was 2.815 Hz, and every fourth frame is displayed in Figure 5A. Each rectangular frame of the image is displayed as a 9030 × 108 $\mu$m rectangle, with the $x$ axis at the center of each frame aligned to the center of the 100 $\mu$m i.d. capillary. Spatial resolution is governed by the size of the effective pixel, $x \times y = 70 \times 7$ $\mu$m. The main peak is seen to be sharp and to have the profile in the $y$ direction expected for a front uniformly distributed in space across the circular cross-section capillary. The frame sequence suggests the presence of a minor trailing component progressing across the window with slightly lower velocity. Processing the images to optimize the velocity as described in UV Area Imaging Detection allowed the velocity of the zone to be determined as 1.15 mm $s^{-1}$ (see Figure 5B). The same optimization routine (data not shown) confirmed that the velocity of the minor component was slightly lower, 1.12 mm $s^{-1}$. The part of the signal that may appear as a minor component corresponds to bacteria and should be considered as a part of the same focusing zone. However, the focusing mechanism is dynamic and there is a continual tension with dispersive processes such as the formation of aggregates of different sizes (and thus different mobilities). This can lead to some peak (or zone) dispersion and fluctuations. Nevertheless, the ITP process succeeds in keeping the bacteria in a zone of a few millimeters width. Figure 5C shows the time-dependent absorbance from frames processed at 1.15 mm $s^{-1}$. The width of the main peak (FWHM) is 0.0026 min, corresponding to 180 $\mu$m. This is a factor 2.6× greater than the 70 $\mu$m spatial resolution of the detector in the flow direction. The total width of the zone (major plus minor peak) is 0.015 min, corresponding to a length of 1.0 mm. The length of the band injected, calculated using Poiseuille's law, was 9.7 mm. Thus, the focusing of the zone over the 27 cm length to the detection window provides a concentration enrichment factor of ~10. Zoom views of the four peaks shown in Figure 4B (data not shown) at the four different detection windows each separated by 15 cm indicate that some bacteria are moving slightly relative to the main peak, but that the ITP process keeps them inside a zone with spatial width of a few millimeters. Because the total area remains constant, it is clear that all the bacteria are kept in the same focused zone without loss of matter but with some local fluctuations in concentration, in the front or in the tail of the main peak.

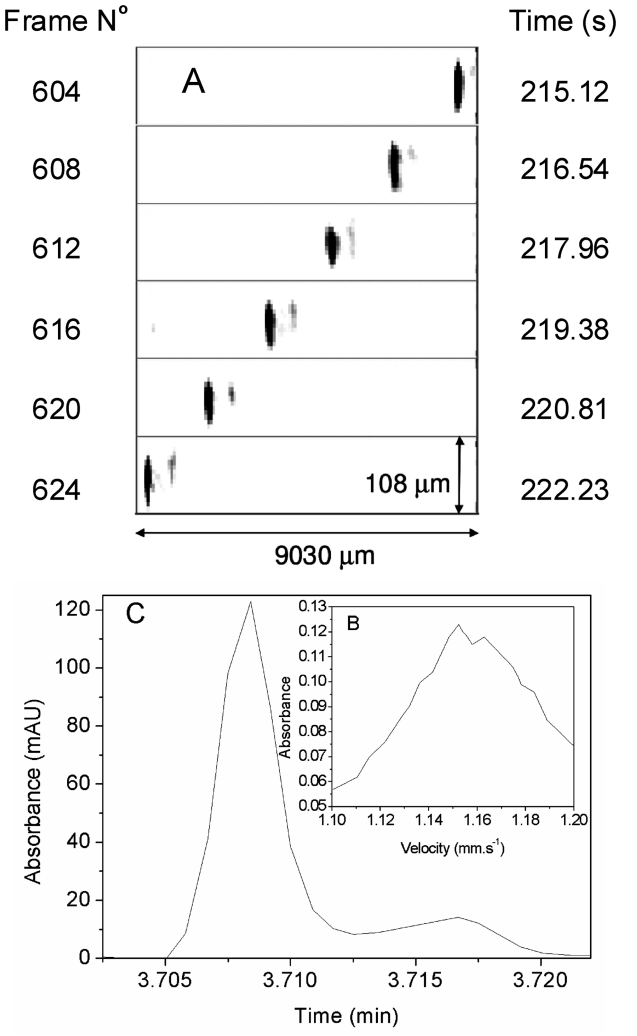


**Figure 5.** UV images and processed frames of the focused *M. luteus* zone moving across the capillary window. Separation conditions: HPC-coated capillary, 80 cm (27 cm to the detector) × 100 $\mu$m i.d. BGE: system D (see Table 1). Applied current: 4 $\mu$A. Hydrodynamic injection: 50 mbar, 5 s. Sample: *M. luteus* at 2.4 × $10^8$ cells/mL diluted in 4.5 mM Tris, 50 mM boric acid. Detection at 280 nm using ActiPix D100 in imaging mode, frame rate 2.82 Hz. (A) Sequence of images showing zone crossing window area (direction of movement right to left, every fourth frame shown). (B) Images processed in frame mode (zero time constant, sample rate 20 Hz) showing optimization of velocity at 1.15 mm $s^{-1}$. (C) Time-dependent absorbance from frames processed at optimum linear velocity.

In order to confirm the mechanism of isotachophoresis, the electrophoretic behavior of small molecules was also investigated under the same conditions. Figure 6A shows the electrophoretic profiles of benzoate (BA) and anthraquinone-1,5-disulfonate (AQDS) in system D. Figure 6B displays the electrophoretic profiles of these two anions at the same concentrations but with $HPO_4^{2-}$ added to the sample. Except for the ITP mode, benzoate and anthraquinone-1,5-disulfonate migrate as broad zones and are separated by $HPO_4^{2-}$ according to their effective mobilities. The zone heights are independent of the solute concentration in the sample and depend only on the concentration of the leading ion ($Cl^-$), the effective mobilities of the ions, and the absorption coefficients at the detection wavelength. The zone widths were found to increase with increasing solute

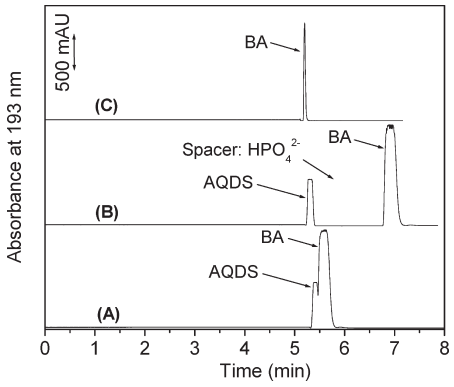


**Figure 6.** Isotachopherograms of three small ions in system D. Experimental conditions: Hydroxypropyl cellulose (HPC)-coated capillary 33.5 cm (25 cm to the detector) × 100 $\mu$m i.d. Electrolytes: system D (see Table 1 for BGE composition). Applied current: 3 $\mu$A. Hydrodynamic injection: 17 mbar, 6 s. Sample: benzoic acid at 0.185 g/L and anthraquinone-1,5-disulfonic acid disodium salt at 0.193 g/L (A), benzoic acid at 0.185 g/L, anthraquinone-1,5-disulfonic acid disodium salt at 0.193 g/L, and $Na_2HPO_4$ at 1.17 g/L (B), and benzoic acid at 0.031 g/L (C). Samples are diluted in Tris (13.6 mM)/boric acid (150 mM) buffer. Abbreviations: benzoate (BA) and anthraquinone-1,5-disulfonate (AQDS).

concentration, as expected by the Kohlrausch regulating function. This contrasts with the observations for *M. luteus* using system C (Figure 3), where a single and sharp peak was observed whatever the concentration of the cells. The difference is likely due to the relatively low number of analytes in the case of bacteria as compared with small ions. For an injection of 87 nL (Figure 4B) and for a 2.5 × $10^8$ cells/mL bacteria concentration, the number of bacteria injected is about 2.2 × $10^4$ cells while for approximately the same injected volume (83 nL in Figure 6) the number of benzoic acid molecules is almost 10 orders of magnitude higher (7.5 × $10^{13}$ in Figure 6B). On lowering the concentration of benzoic acid by a factor of 6 the broad zone observed in Figure 6A and 6B was found to change into a narrow peak as seen in Figure 6C.

**From ITP to CZE.** Figure 7A displays electropherograms in ITP mode and for sequential ITP-CZE obtained for two small anions, benzoate (BA) and anthraquinone-2-sulfonate (AQS). Figure 7B shows the corresponding results of ITP and ITP-CZE for *E. carotovora* (model of Gram− bacteria). These electropherograms were obtained using the imaging UV detector as described in UV Area Imaging Detection. For ITP, the electrolytes were those of system D. For ITP-CZE, the ITP mode was performed using system D for 5 min at constant current (3 $\mu$A), and after 5 min, the inlet vial containing BGE1 was removed and replaced by an inlet vial containing BGE2, and the separation was continued at constant voltage (−30 kV), as in zone mode. Under these conditions, the interface between the leading and the terminating compartment becomes diffuse, and the leading electrolyte penetrates progressively into the terminating electrolyte. When the leading ions catch up with the analyte ions, ITP ceases and makes way to CZE which allows separation of the compounds. In the ITP mode, benzoate and anthraquinone-2-sulfonate migrate at the same velocity as contiguous zones during the whole isotachophoretic process (Figure 7A). For *E. carotovora* (Figure 7B), only one single and sharp peak was observed, as for *M. luteus*. For sequential ITP-CZE, Figure 7A shows that for this system, the separation of benzoate and anthraquinone-2-sulfonate begins at

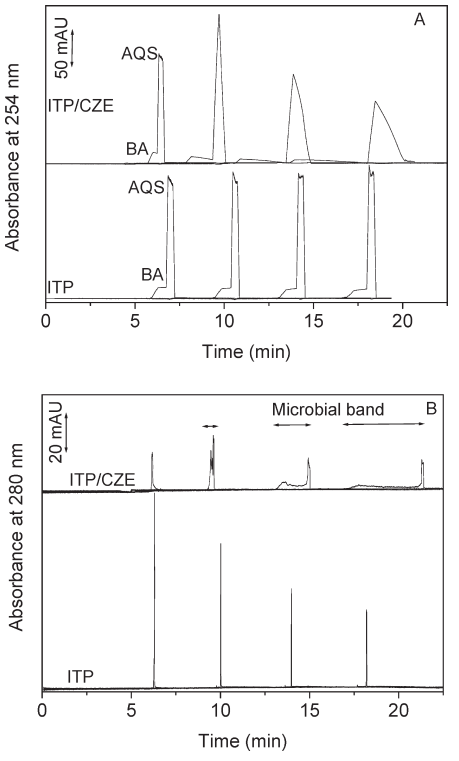


**Figure 7.** ITP and sequential ITP-CZE with four detection windows in system D for two small molecules (A) and *E. carotovora* (B). Experimental conditions: Hydroxypropyl cellulose (HPC)-coated capillary, 109 cm with three loops and four detection windows (27.5 cm to the 1st, 42.5 cm to the 2nd, 57.5 cm to the 3rd, and 72.5 cm to the 4th detection window) × 100 $\mu$m i.d. Electrolyte (ITP mode): System D. Applied current: 3 $\mu$A. Electrolyte (sequential ITP-CZE): System D during 5 min and then the BGE1 of system D was replaced by the BGE2 of the same system (see Table 1 for BGE compositions). Applied current/voltage: 3 $\mu$A for 5 min and −30 kV after 5 min. Multiplexed detection using ActiPix D100 UV area imaging detector at 280 nm. Samples: *E. carotovora* at 5.5 × $10^7$ cells/mL (A), benzoic acid at 0.792 g/L and anthraquinone-2-sulfonic acid sodium salt at 0.258 g/L (B). Both samples are diluted in 13.6 mM Tris/150 mM boric acid buffer. Hydrodynamic injection: 50 mbar, 7 s. Abbreviations, benzoate (BA) and anthraquinone-2-sulfonate (AQS).

around 10 min. For *E. cloacae*, after 10 min, the focused zone becomes broader at the successive windows, demonstrating that the ITP mode is required to keep the band focused. However, it is worth noting that the trailing edge is always sharp for *E. carotovora*.

**Focusing in a Range of ITP Background Electrolytes and Computer Simulation of ITP Process.** The BGE systems used in this work are not commonly used in isotachophoresis. Generally, the terminating electrolyte is only in the terminating compartment and is not present in the leading compartment. In this work, borate is present in both compartments, but at a higher concentration in the terminating compartment due to the higher pH. A computer simulation (Simul 5.0[29]) was carried out using the actual concentrations in system D to assist in understanding the focusing mechanism. Figure 8 displays simulation of the distribution of pH, conductivity, and ion concentrations as a function of position in the capillary at an early stage in the ITP experiment. The results obtained by computer simulation correspond to those obtained in practice with system D using benzoate and anthraquinone-1,5-disulfonate as analytes (Figure 6A).

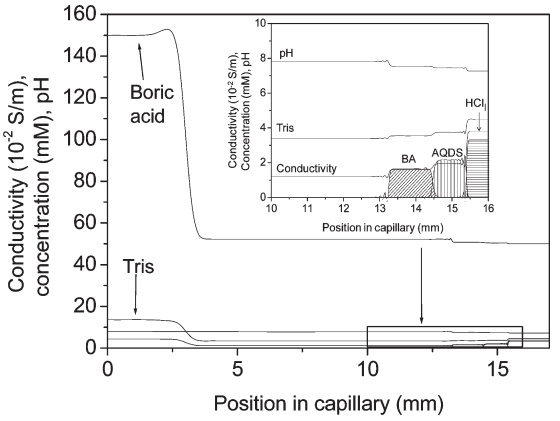


**Figure 8.** Simulation of the distribution of conductivity, ion concentrations, and pH for the ITP experiments shown in Figure 6A, as a function of the position in the capillary. Simulation conditions: times courses: 22.427 s. BGE: system D. Sample: benzoic acid (BA) at 2 mM and anthraquinone-1,5-disulfonic acid (AQDS) at 2 mM diluted in 13.6 mM Tris/150 mM boric acid buffer. Other conditions: see ITP Computer Simulation.

Benzoate and anthraquinone-1,5-disulfonate migrate as broad zones according to their effective mobilities and at the same velocity. Thus, as shown in the insert of Figure 8, the conductivities in the different zones increase as the mobilities increase. Under the conditions of constant current, the local field strengths decrease as the conductivities increase.

Two commonly used isotachophoresis buffer systems were also tested to confirm that cell focusing was due to ITP. The first background electrolyte system[41] was constituted by Tris (9.32 mM)/MES (5.09 mM) (pH 8.04) as terminating electrolyte and Tris (5.72 mM)/HCl (3.04 mM) (pH 8.05) as leading electrolyte. The second system[42] was constituted by Tris (4.52 mM)/TAPS (8.60 mM) (pH 7.93) as terminating electrolyte and Tris (5.20 mM)/HCl (3.04 mM) (pH 7.93) as leading electrolyte. These systems both gave similar results for the focusing of bacteria as in system D (results not shown). However, it is well-known that the solutions of bacteria can change with time.[12] If different electrolyte systems can be used for the ITP focusing of bacteria, electrolyte system D based on boric acid is a good candidate due to the bacteriostatic properties[43] that can help maintain a constant concentration of bacteria.

## ■ CONCLUSION

An electrophoretic method has been developed that allows detection of bacteria in a narrow zone at close to physiological pH and does not require addition of any polymer additive, surfactant, or strong complexing reagent such as EDTA. During this work, four genera of bacteria have been tested and analyzed successfully. This method allows the quantification of bacteria because the peak area is linearly dependent on the concentration. Very good linearity was obtained in these electrophoretic conditions, with correlation coefficients of 0.999 for peak height and 0.998 for peak area of *M. luteus*. The mechanism of focusing was clearly demonstrated as isotachophoresis, and the use of a UV area imaging detector for visualization of the bacterial zone at four windows in a looped capillary demonstrated that the ITP steady state was rapidly obtained when using appropriate electrolyte compositions. Variants of the method have been demonstrated for both bare and hydroxypropyl cellulose-coated fused

silica capillaries. Migration times are less than 3 min when using short (33.5 cm), bare, fused silica capillaries, while maintaining very low electrical currents in order to minimize any Joule heating in the capillary and the lysis of bacteria. This method could potentially be applied for the detection of very low concentrations of bacteria in microbial food contamination or micro-organisms in biological samples.

## AUTHOR INFORMATION

### Corresponding Author

*Tel: +33-4-6714-3427. Fax: +33-4-6763-1046. E-mail: hcottet@univ-montp2.fr.

## ACKNOWLEDGMENT

H.C. gratefully acknowledges the support from the Région Languedoc-Roussillon for the fellowship "Chercheurs d'Avenir". T. Z. thanks the University of Montpellier 2 for a postdoctoral grant from the Scientific Council. We also thank COLCOM for funding a fellowship for F.O., the ANR Dendrimat (grant reference ANR-096MAPR-0022-03), and Yorkshire Forward for support through a Development Grant to Paraytec Ltd. (grant reference YHF/02803/RD09).

## REFERENCES

(1) World Health Organization. *Infectious diseases report: Removing obstacles to healthy development*; Atar: Geneva, Switzerland, 1999.
(2) World Health Organization. *Cholera Outbreak: Assessing the outbreak response and improving preparedness*; Report No. WHO/CDS/CPE/ZFK/2004, WHO Press: Geneva, Switzerland, 2004.
(3) Bartram, J.; Chartier, Y.; Lee, J. V.; Pond, K.; Surman-Lee, S. *Legionella and the prevention of legionellosis*; World Health Organization Press: Geneva, Switzerland, 2007.
(4) Black, J. G. *Microbiology principles and applications*; Prentice-Hall: Upper Saddle River, NJ, 1996.
(5) Stinson, S. C. *Chem. Eng. News* **1999**, *77*, 36–38.
(6) Hobsen, N. S.; Tothill, I. E.; Turner, A. F. P. *Biosens. Bioelectron.* **1996**, *11*, 455–477.
(7) Hjertén, S.; Elenbirg, K.; Kilar, F.; Liao, J. *J. Chromatogr.* **1987**, *403*, 47–61.
(8) Buszewski, B.; Klodzińska, E.; Dahm, H.; Różycki, H.; Szeliga, J.; Jackowski, M. *Biomed. Chromatogr.* **2007**, *21*, 116–122.
(9) Buszewski, B.; Klodzińska, E. *Electrophoresis* **2008**, *29*, 4177–4184.
(10) Dai, D.; Chen, Y.; Qi, L.; Yu, X. *Electrophoresis* **2003**, *24*, 3219–3223.
(11) Buszewski, B.; Szumski, M.; Klodzińska, E.; Dahm, H. *J. Sep. Sci.* **2003**, *26*, 1045–1049.
(12) Armstrong, D. W.; Schulte, G.; Schneiderheinze, J. M.; Westenberg, D. J. *Anal. Chem.* **1999**, *71*, 5465–5469.
(13) Jackowski, M.; Szeliga, J.; Klodzinska, E.; Buszewski, B. *Anal. Bioanal. Chem.* **2008**, *391*, 2153–2160.
(14) Garcia-Canas, V.; Cifuentes, A. *Electrophoresis* **2007**, *28*, 4013–4030.
(15) Girod, M.; Armstrong, D. W. *Electrophoresis* **2002**, *23*, 2048–2056.
(16) Shintani, T.; Yamada, K.; Torimura, M. *FEMS Microbiol. Lett.* **2002**, *210*, 245–249.
(17) Yu, L.; Li, S. M. Y. *J. Chromatogr. A* **2007**, *1161*, 308–313.
(18) Schneiderheinze, J. M.; Armstrong, D. W.; Schulte, G.; Westenberg, D. J. *FEMS Microbiol. Lett.* **2000**, *189*, 39–44.
(19) Hoerr, V.; Stich, A.; Holzgrabe, U. *Electrophoresis* **2004**, *25*, 3132–3138.
(20) Rodriguez, M. A.; Lantz, A. W.; Armstrong, D. W. *Anal. Chem.* **2006**, *78*, 4759–4767.
(21) Bao, Y.; Lantz, A. W.; Crank, J. A.; Huang, J.; Armstrong, D. W. *Electrophoresis* **2008**, *29*, 2587–2592.
(22) Petr, J.; Jiang, C.; Sevcik, J.; Tesarova, E.; Armstrong, D. W. *Electrophoresis* **2009**, *30*, 3870–3876.
(23) Horká, M.; Horký, J.; Matoušková, H.; Šlais, K. *J. Chromatogr. A* **2009**, *1216*, 1019–1024.
(24) Crombrugge, J.; Waes, G. *Methods for Assessing the Bacteriological Quality of Raw Milk from the Farm*; Heeschen W.: Brussels, Belgium, 1991.
(25) Shen, Y.; Smith, R. D. *J. Microcol. Sep.* **2000**, *12*, 135–141.
(26) Shen, Y.; Berger, S. J.; Anderson, G. A.; Smith, R. D. *Anal. Chem.* **2000**, *72*, 2154–2159.
(27) Kulp, M.; Urban, P. L.; Kaljurand, M.; Bergström, E. T.; Goodall, D. M. *Anal. Chim. Acta* **2006**, *570*, 1–7.
(28) Urban, P. L.; Goodall, D. M.; Carvalho, A. Z.; Bergström, E. T.; Van Schepdael, A.; Bruce, N. C. *J. Chromatogr. A* **2008**, *1206*, 52–63.
(29) Hruška, V.; Jaroš, M.; Gaš, B. *Electrophoresis* **2006**, *27*, 984–991.
(30) Zheng, J.; Yeung, E. S. *Anal. Chem.* **2003**, *75*, 818–824.
(31) Madigan, M. T.; Martinko, J. M. *Brock Biology of Microorganisms*; Prentice Hall: Upper Saddle River, NJ, 2005.
(32) Armstrong, D. W.; Girod, M.; He, L.; Rodriguez, M. A.; Wei, W.; Zheng, J.; Yeung, E. S. *Anal. Chem.* **2002**, *74*, 5523–5530.
(33) Survay, M. A.; Goodall, D. M.; Wren, S. A. C.; Rowe, R. C. *J. Chromatogr. A* **1996**, *741*, 99–113.
(34) Landolt-Börnstein. *Zahlenwerte und Funktionen aus Physik-Chemie-Astronomie-Geophysik und Technik*; Springer: Berlin, Germany, 1960.
(35) Kartsova, L. A.; Bessonova, E. A. *J. Anal. Chem.* **2008**, *64*, 340–351.
(36) Jucker, B. A.; Harms, H.; Zehnder, A. J. B. *J. Bacteriol.* **1996**, *178*, 5472–5479.
(37) Moses, N.; Rouxhet, P. G. *J. Microbiol. Methods* **1987**, *6*, 99–112.
(38) Riaz, A.; Chung, D. S. *Electrophoresis* **2005**, *26*, 668–673.
(39) Kvasnička, F. *Electrophoresis* **2000**, *21*, 2780–2787.
(40) Williams, B. A.; Vigh, G. *Anal. Chem.* **1996**, *68*, 1174–1180.
(41) Breadmore, M. C.; Quirino, J. P. *Anal. Chem.* **2008**, *80*, 6373–6381.
(42) Chen, Y.; Zhang, L.; Xu, L.; Lin, J. M.; Chen, G. *Electrophoresis* **2009**, *30*, 2300–2306.
(43) Crann, A. G.; Myres, A. W.; Green, D. W. *Regul. Toxicol. Pharmacol.* **1997**, *26*, 271–280.